Multistep partitioning causes significant stable carbon and hydrogen isotope effects during volatilization of toluene and propan-2-ol from unsaturated sandy aquifer sediment

Sarah Zamane, Didier Gori, Patrick Höhener

Multistep partitioning causes significant stable carbon and hydrogen isotope effects during volatilization of toluene and propan-2-ol from unsaturated sandy aquifer sediment

Sarah Zamane, Didier Gori and Patrick Höhener*

Aix Marseille University – CNRS, UMR 7376, Laboratory of Environmental Chemistry, Marseille, France

*Corresponding author. patrick.hohener@univ-amu.fr

Chemosphere **251**: 126345. 10.1016/j.chemosphere.2020.126345.

Graphical abstract

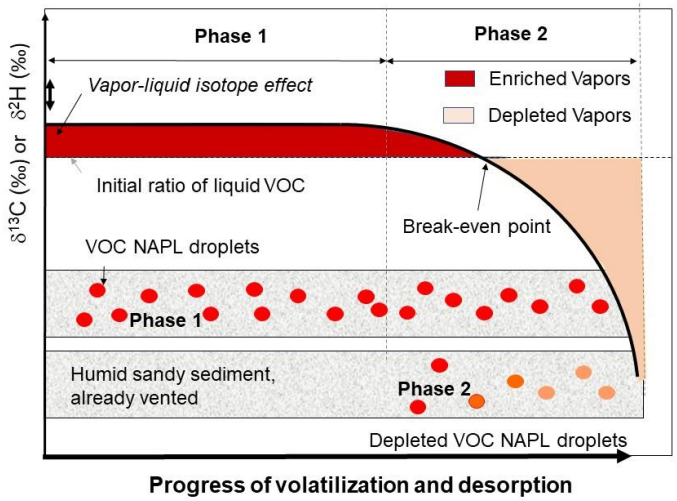

Highlights

- Compound-specific stable isotope analysis is used for monitoring of soil venting
- Volatilization of toluene and propan-2-ol were studied with C and H isotopes
- Column experiments with aquifer sediment yielded large isotope effects (IE)
- A numerical model based on multistep vapor-liquid partitioning reproduces these IE
- The isotope shifts found here are larger than shifts created by equilibrium processes

Abstract

This study aimed at investigating whether stable isotopes can be used to monitor the progress of volatile organic compounds (VOCs) volatilization from contaminated sediment during venting. Batches of a dry aquifer sediment were packed into stainless steel HPLC columns, humidified with distilled water and later contaminated by either liquid toluene or propan-2-ol. The VOCs were then volatilized by a stream of gas at room temperature, and the concentrations and stable isotope ratios of gaseous VOCs were recorded by isotope-ratio mass spectrometry. During early stages of volatilization of toluene, the isotope ratios $\Delta\delta^{13}C$ shifted to more negative values by about -3 to -5 ‰ and the $\Delta\delta^{2}H$ by more than -40 ‰, while the concentration remained at or near initial saturated vapor concentration. Depletion of the isotope ratios in the gas was explained by the vapor-liquid fractionation process, which is amplified by successive self-partitioning steps of gaseous VOC into remaining liquid VOC. For propan-2-ol the carbon isotope shift was negative like for toluene, whereas the H shift was positive. Hydrogen bonding in the liquid propan-2-ol phase causes a normal vapor-liquid H isotope effect which was described already in classical literature. The isotope shifts in the present experiments are larger than previously reported shifts due to phase-change processes and reach the magnitude of shifts usually observed in kinetic isotope fractionation.

Keywords

Carbon-13, Deuterium, Partitioning, Soil venting, Remediation

1. Introduction

Spills of volatile organic compounds (VOCs) such as e.g. petroleum products or solvents to soils are a frequent environmental problem that needs corrective actions. In situ soil venting or bioventing is a widespread technique to treat sites with contaminations in the unsaturated zone (Aelion and Kirtland, 2000; Ostendorf and Kampbell, 1990; Rathfelder et al., 1995). In order to better predict its feasibility, the understanding of rates controlling volatilization and desorption are needed. Numerous investigations have already contributed to a better understanding of these mechanisms (Allen-King et al., 2002; Balseiro-Romero et al., 2018; Brusturean et al., 2007; Delle Site, 2001). Grathwohl and Reinhard (1993) performed pioneering work on the volatilization and desorption of trichloroethene from aquifer sediments and found that diffusion at the grain scale exhibits a rate-limiting control for the desorption process at late stages of remediation.

Compound-specific isotope analysis (CSIA) is a now established tool for monitoring of remediation progress (Thullner et al., 2012; Vogt et al., 2016). In VOCs from petroleum, stable carbon and hydrogen isotopes can be used to assess the progress of isotope-fractionating reactions. Applications were reported for tracking processes which lead to significant isotope fractionation. These are bond-breaking processes on one hand (Elsner, 2010) and gas-phase diffusion-controlled processes on the other hand (Bouchard et al., 2008; Höhener et al., 2008). Both processes are subject to kinetic isotope effects, remove preferentially the light isotopes and lead to isotopic enrichment of the remaining pollutant (normal isotope effect, IE). Besides these two kinetic fractionation effects, equilibrium-based phase-transfer processes like sorption, desorption and partitioning (neat liquid – air or water-air) were reported to create negligible (Schuth et al., 2003; Slater et al., 2000) or only small fractionations for both, C and H (Imfeld et al., 2014; Kopinke et al., 2005) (see Tables S4+S5). For toluene, the largest phase-transfer isotope shifts so far observed

caused by multistep sorption to various sorbents were +1.4 ‰ for ^{13}C and +12 ‰ for ^{2}H (Imfeld et al., 2014). These isotope shifts were qualified as "insignificant" compared to shifts by bond-breaking reactions or by gas-phase diffusion (Imfeld et al., 2014). For both isotopes, the IE was inverse meaning that the heavy isotopologue adsorbed less strongly than the light isotopologue. Such an inverse behavior of apolar compounds is well known, especially for deuterated compounds, and can lead to chromatographic separation of fully deuterated hydrocarbons on gas chromatographic columns, with first elution of the heavy compounds (Höhener and Yu, 2012; Morasch et al., 2001). It should be noted here that passive volatilization of apolar COVs includes diffusive fractionation in a stagnant boundary layer which can overcome the inverse vapor-liquid effect to result in an overall normal effect (Julien et al., 2015).

The objective of our work was to use CSIA in order to get a better insight into the process significance of forced volatilization of VOCs from unsaturated aquifer sediments. To this end, the fractionation of isotopes occurring during volatilization were quantified in column experiments and compared to previously known fractionations for biodegradation, diffusion and phase-change processes. Toluene was chosen as a typical apolar pollutant, and for comparison, the polar solvent propan-2-ol was added. For both compounds vapor-liquid isotope effects for C and H are known (Table S5).

2. Material and methods

Toluene and propan-2-ol (both >99.8 purity) were purchased from Sigma-Aldrich. The aquifer sediment was from an uncontaminated quarry in the Crau aquifer plain (Ponsin et al., 2015). The fraction > 2 mm was removed by dry sieving and the material was then sieved wet on a mesh of 0.124 mm rinsed with distilled water and dried at 110°C. Its characteristics are given in the table S3. A stainless steel HPLC column of 25 cm length and 4.6 mm internal diameter was emptied and

filled with 6.6 grams of dry aquifer sediment, using small packs of glass wool at both ends to retain the sand in between.

2.1 Contamination procedure

A volume of 360 μL of distilled water was pipetted into the column which was then closed with two plugs and incubated overnight at 80°C in order to distribute water vapor uniformly. After cooling to room temperature, a known volume of liquid VOC (Table S1) was inserted on the top of the column, which was closed again by plugs and heated to 80°C during 18 h. After cooling to 25°C, condensing the VOCs as liquid phase, the column was weighted. Then the column was filled homogeneously with humid aquifer sediment containing liquid toluene drops and toluene in vapor, aqueous phase and adsorbed to sediment. The volumetric fluid contents were 0.108 for toluene, 0.087 for water and 0.234 for air for the experiment shown in Figure 1. Thereafter volatilization was studied recording stable carbon isotope ratios. When no more VOC vapors left the column, the column was disconnected, vented, then re-humified and re-contaminated with VOC in identical manner. Volatilization was then again studied recording hydrogen isotopes ratios in the GC-IRMS. Similar experiments were performed with other HPLC columns of the same dimensions but without adding water in order to avoid microbial degradation. The columns were closed by plugs, and the VOC could sorb onto the sediments for variable periods of 30 minutes to up to 10 days at room temperature.

2.2 Volatilization experiments

The HPLC columns were connected in horizontal position to polyether-etherketone (PEEK) tubing and volatilization was performed with a stream of Helium gas (different flow rates were tested from 3 to 12 mL min^{-1}, corresponding to 0.5 to 2 mL cm^{-2} min^{-1}). Volatilization by air was avoided since it could promote biodegradation. Four experiments were also performed with N_2 gas in order

to test a gas more similar to air. The gas flow rates were controlled via the entry pressures which ranged from 1.5 to 2 atm. The first volumes of the gas stream were discarded if liquid VOC emerged. The gas stream was then led through a 6 mL headspace autosampler vial in a rack of an autosampler (Triplus, Thermo-Fisher Scientific) heated to 60°C. The flow rate of the gas was monitored at the vent tube using a soap flow meter. Automated injections from this vial flushed continuously by the vented VOCs were performed with a gas-tight syringe into a GC-C-IRMS system composed of the Trace GC connected via Isolink II interface to a Delta V Advantage Isotope Ratio Mass Spectrometer (all from Thermo Fisher Scientific). The experimental scheme and the running conditions are given in the SI, Figs. S1+2 and Tab. S2. VOC concentrations were recorded using the amplitude of mass 44 of CO_2 in IRMS in combustion mode or the amplitude of mass 2 of H_2 in pyrolysis mode.

The measured delta $\delta^{13}C$ or $\delta^{2}H$ (‰) were calculated following eq. (1):

$$\delta\ (‰) = \frac{R_{sample} - R_{standard}}{R_{standard}} . 1000 \qquad (1)$$

With R_{sample} being the ratio of the sample and $R_{standard}$ the abundance ratios of the international standards (VPDB, 0.0112372 or VSMOW, 1.5575E-4). Values were corrected using two secondary lab standards, toluene and benzene, running on GC-C-IRMS which were themselves compared to primary standards (VSMOW, NBS-22 from IAEA, and urea from Thermo Scientific) by EA-IRMS. The linearity and uncertainty of the measured isotope ratios were checked by additional injections of toluene from vials with different vapor concentrations and are shown in Fig. S3 which shows also the analytical errors of the δ values (± 0.5 ‰ for ^{13}C and (± 5.0 ‰ for ^{2}H) The pore volumes of the sand-filled chromatographic columns were determined from subtracting sediment volume from total column volume after each experiment, and the gas flow rates were transformed to number of pore volumes (PVs) flushed during each run. The

results from one experiment were also displayed as isotope ratios as a function of mass loss, using the Rayleigh plot approach (eq. 2). If data plotted with equation 2 fall on a straight line, the slope is equivalent to the enrichment factor ε.

$$1000 * \ln\left(\frac{\delta+1000}{\delta_0+1000}\right) = \varepsilon \ln\left(\frac{M}{M_0}\right) \quad \text{(eq. 2)}$$

2.3 Modelling

A numerical model was created in order to investigate whether a multistep vapor-liquid IE is a plausible cause of our observations. The column was schematically represented as a sequence of stirred non-aqueous liquid solutions (NAPLs) containing light and heavy toluene isotopologues which partition into a gas stream. The two isotopologues were handled as two different compounds, and the theoretical vapor pressure was attributed to light isotopologues whereas the vapor pressure for the heavy isotopologues was derived using an IE from the literature.

The model parameters are given in the table S6. The model is based on PHREEQC (USGS, 2002) and its code is presented in the SI.

3. Results

3.1 Volatilization of toluene

A total of 31 volatilization experiments were done, and the conditions which were tested, and the rationales for choosing each condition were given in Table S1. The first experiment shown here is one for a sediment contaminated with 0.39 g of liquid toluene for a duration of 18 hours (Figure 1). The evolution of the vapor concentration, expressed as amplitude 44, and the isotope ratio $\delta^{13}C$, can be described as happening in four distinct phases. In phase 1, during the first 1100 PVs, both amplitude and $\delta^{13}C$ did not change significantly. In phase 2, lasting about 300 PVs, the amplitude stayed constant, whereas $\delta^{13}C$ values decreased from the initial -26,9 ‰ to -28.7 ‰. Then, in a

third phase, lasting about 500 PVs, the amplitude dropped quickly from more than 2500 to less than 200 mV, while $\delta^{13}C$ values increased back to the initial values. During the last phase 4, the amplitude 44 sank to less than 50 mV, while $\delta^{13}C$ could not be measured anymore.

The isotope data of figure 1A are also shown as a plot in function of mass loss using equation 2 (Fig S4). No straight line could be established in that plot, as in phase 1 mass is lost without any marked change in isotope ratios, and in phase two isotope ratios are changing without much mass loss.

The evolution of stable hydrogen isotope ratios in the experiment repeating the conditions shown in Figure 1A is shown in Figure 1B. The amplitude 2 stayed near the initial value of 8000 mV until 1370 eluted PVs and dropped then sharply to less than 200 mV. The $\delta^{2}H$ values stayed unchanged until about 750 eluted PVs and then decreased gradually from -35 ‰ to -71 ‰ at 1370 PVs and were not measurable thereafter. The experiment observed with IRMS set to hydrogen mode showed thus almost the same behavior as for carbon in phases 1 and 2, with the exception that the magnitude of isotope shift was larger in the hydrogen experiment. Phases 3 and 4 could not be assessed due to the lack of isotope data after the too large drop in amplitude (Fig. 1B).

In order to understand the causes of these behaviors, a total of > 40 other experiments were performed. The factors which were varied were 1) increasing time of sorption (only performed in dry sediments in order to avoid biodegradation); 2) decreasing mass of VOC; 3) variation of gas flow rate; and 4) use of N_2 instead of He. Increasing the contact time of toluene to sediment to up to 10 days was showing an equal behavior during all phases. Also, replacement of the flushing gas He by N_2 led to equal results both for C and H (data not shown). However, it was found that the initial mass of toluene had a significant effect on the start of the drop of amplitude. This could best be visualized by experiments with column (Figure 2 and Fig. S4).

In Figure 2, a proportionality between VOC mass and number of PVs is evident in the drops of the amplitudes. The increase of the flow rate from 6 to 12 mL min^{-1} retarded the drop of the amplitude slightly. The magnitude of the drop of the isotope ratio, in contrast, was not found to give a systematic trend with initial mass. It was found to depend on whether the timing of the last data point was close to the drop of the amplitude.

3.2 Volatilization of propan-2-ol

In order to study the evolution of stable isotope ratios in another more polar VOC, propan-2-ol was selected. Figure 3 shows the evolution of $\delta^{13}C$ and $\delta^{2}H$ in propan-2-ol (~0.3 g) during volatilization/desorption with He for a contamination of dry sediment aged for 12 hours.

The evolution of $\delta^{13}C$ in propan-2-ol (Fig. 3A) was like that of toluene (Fig. 1), with an isotope shift of – 3 ‰. In contrast, the $\delta^{2}H$ showed a shift to more positive values in the final stage of phase 2, with a rise of approximately +20 ‰.

3.3 Modelling

In order to better understand the influence of VOC mass and other factors on the volatilization behavior, a numerical model was created. Results from the model for carbon isotopes in toluene are shown in Figure 4. A base case scenario assumed that the modeled column contained 0.26 g of liquid toluene, distributed in 20 cells. Additional model runs were performed for other toluene masses (Fig. 4A), for other numbers of cells forming the column (Fig. 4B), for other dispersivities (Fig. 4C) and for variations in the vapor-liquid IE (Fig. 4D). As shown in Fig. 4, the variation of VOC mass had the largest influence on the modeled isotope ratios, followed by the variation of the vapor-liquid IE. The number of cells and the dispersivity had little or insignificant influence on the results.

200

201 # 4. Discussion

202 ## 4.1 Toluene

203 These experiments reveal significant isotope shifts of C and H during volatilization of toluene
204 from unsaturated sandy aquifer sediment. The shifts for both C and H occur in phase 2 of venting,
205 during which the vapor concentration was near saturation. A shift back to initial isotope ratios
206 occurred later for $\delta^{13}C$ but could not be observed for $\delta^{2}H$ because the sensitivity of the IRMS is
207 lower for ^{2}H than for ^{13}C. This shift back to initial $\delta^{13}C$ was accompanied by a large drop of
208 vapor concentrations. Before the drop, vapors were supposed to be generated from liquid VOC,
209 while after it they were supposed to be generated by desorption from sediment or by
210 volatilization from water.
211 The isotope shifts for C and H were larger than shifts observed for the volatilization of neat
212 compounds in beakers (summarized in Tables S4 and S5 in SI). The discussion of the results will
213 focus mainly on IEs observed during phases 1 and 2 of the experiments with respect to vapor-liquid
214 partitioning, because data for phases 3 and 4 are only available for carbon. During phases 1+2,
215 liquid toluene was present in the column and the vapor concentration at the outlet was at or near
216 saturation point. All known vapor-liquid IEs for both studied VOCs are listed in tables S4+S5. The
217 equilibrium vapor-liquid IEs for toluene was reported as being +0.2 ‰ for ^{13}C. (Harrington et al.,
218 1999) Similar values of +0.3 ‰ and +0.4 ‰ were obtained for low-pressure evaporation at room
219 temperature and for distillation at 110°C, respectively (Julien et al., 2017). For ring-
220 monodeuterated toluene a value of +7.0 ‰ was reported (Kiss et al., 1972). Both heavy
221 isotopologues ^{13}C and ^{2}H are more volatile than their lighter counterparts because of the lower
222 molar volume of the liquid phase causing more collisions in the liquid which creates a higher vapor

pressure (Bartell and Roskos, 1966). A preferential volatilization of heavier toluene is thus occurring during volatilization from the liquid phase into the column gas phase. The gas flow in the column is dominated by advection and no diffusion should control the phase-transfer. This is different from volatilization from an open beaker in a fume hood where a stagnant diffusive gas boundary layer between the liquid phase and the turbulent air is present which causes an additional diffusive IE, as discussed in detail in previous works. (Julien et al., 2017; Kuder et al., 2009). Without stagnant boundary layer, it can be postulated that the vapor is at any point in the column enriched compared to the liquid VOC, and that the difference corresponds to the vapor-liquid IE. While both light and heavy toluene volatilize and move through the column, the light toluene has a larger tendency to partition back into the liquid phase along the column. Initially, the loss of liquid phase is high at the column inlet, and low or zero near the column outlet. As volatilization proceeds during phase 1, the liquid phase volatilizes and disappears progressively along the column, and the remaining liquid phase near the column outlet gets gradually depleted by the back-partitioning of light isotopologues. The number of pore volumes which form phase 1 for a given constant flow rate depends intuitively on the VOC liquid mass since the saturated vapor concentration at the outlet is invariant. Phase two starts when this isotopically depleted liquid phase starts to volatilize, and it ends when the column does not contain any depleted liquid toluene anymore. This point is easily identified because the vapor concentration drops drastically.

For carbon, the isotope ratios then returned to near initial values in phase 3 during elution of toluene desorbed from sediment (Fig. 1A). The drop of vapor concentrations during phase 3 and 4 followed a trend described by (Grathwohl and Reinhard, 1993) as a desorption rate governed by intra-particle diffusion and sorption. For short desorption times, the decrease in concentration or flux follow both a linear slope on a diagram log C/C0 or log flux versus PVs (Grathwohl and

Reinhard, 1993). Our vapor data converge to such a linear slope at the end of phase 4 in the experiment (Fig. 1).

The evolution of the isotope ratio during phases 1+2 is not related to the mass loss in the column by a Rayleigh-type evolution (Fig. S4) since during phase 1 mass is lost without any marked change in isotope ratio. Therefore, no Rayleigh-type concept can be applied to quantify enrichment factors.

4.2 Propan-2-ol

This compound is more polar but with a slightly higher volatility than toluene, with a vapor pressure of 5.8 kPa compared to the one of toluene of 3.8 kPa (Broholm et al., 2005) As an alcohol, hydrogen bonds interfere in its liquid. Therefore, the vapor-liquid IE for H is normal and not inverse like for toluene (Tab. S5). In contrast, for carbon the IE is inverse (Julien et al., 2017). Our experiments (Figure 3) yielded a clear opposite IE between C and H, which confirmed that the vapor-liquid IE is the main cause for the isotope shifts in the column experiments. Classical data on vapor pressure IE of different propan-2-ols having deuterium at different positions of the molecule are available (Tab. S5) but do not allow to estimate the magnitude of the deuterium IE at natural abundance ratios. For example, when deuterium was bound to O, a huge normal IE was observed whereas when D was bound to a C the IE was smaller but remained normal.

4.3 Modelling

The results of the model developed for this study (Fig. S5) show the same type of behavior like that observed in the experiments for the phases 1+2 of forced volatilization. The mass of VOC influences the number of pore volumes that need to be vented but does not influence the isotope shift. This agrees with observations in Fig. 2. In contrast, the magnitude of the vapor-liquid IE directly influences the magnitude of isotope shift. In our experiments, the experimental shifts for carbon were higher than the one modeled with a vapor-liquid IE of +0.2 permille in the base case

scenario. This suggests that the true vapor-liquid IE is maybe somewhat higher than 0.2 permille. However, increasing the number of stirred model compartments (cells) increases its maximum isotope shift also slightly at the end of phase 2, while it retards the onset of the isotope shift. As depicted in the graphical abstract, an excess of heavy isotopologues is eluted during phase 1, whereas an excess of light isotopologues follows in phase 2. At its end, when liquid VOCs is gone, the isotope balance is closed. A break-even point separates the two regimes depicted in blue and orange in the graphical abstract. The position of this point depends on the number of stirred solutions chosen in the model. The way of packing the columns affects this number. Figure 1B shows, however, that the variation of isotope shifts is not strongly affected by this number. No sorption or intra-particle diffusion was incorporated in the model. Therefore phases 3+4 were not represented. This will be the objective of future studies. At the beginning of phase 3, when desorption starts, it is plausible that the isotope ratio shifts back to near the initial ratio (Fig. 1) since both light and heavy isotopologues underwent almost equal sorption. Entering phase 4 of the experiment, intra-particle diffusion and desorption might change isotope ratios progressively and this needs to be analyzed with a better resolution.

4.4 Environmental implications

Soil venting and bioventing of petroleum products targets mainly monoaromatic hydrocarbons like toluene and benzene. In the following, the results of our study on toluene are compared to all other IEs potentially occurring during soil bioventing which were reviewed in a recent publication (Bouchard et al., 2018) (Fig. 5).

As shows Figure 5, biodegradation causes isotope enrichment for both isotopes in the remaining toluene, whereas volatilization from water causes enrichment only in hydrogen. Volatilization of NAPL was known to cause depletion in H isotopes, and either depletion or enrichment in carbon

isotopes. This depends whether diffusion is involved: volatilization from a buried NAPL in soil was known to cause C enrichment by diffusion (Bouchard et al., 2008a+b) whereas volatilization of a NAPL exposed to windy air can lead to depletion in C isotopes when the diffusive boundary layer is absent. Our results showed all in depletion of both isotopes and lie in the same area of the graph like the NAPL volatilization in turbulent air, but the overall shifts of our results are larger due to multistep volatilization and back-partitioning.

5. Conclusions

In conclusion, this study finds isotope shifts for carbon and hydrogen exceeding previously known shifts for equilibrium-based phase-transfer processes of the investigated VOCs. The shifts are in the order of magnitude of shifts created by kinetic isotope effects. The findings give new insights in the monitoring of the remediation of soils contaminated by VOCs by means of venting or bioventing. More work is needed for extending the experimental scale to 3 dimensions, and for the study of late stages of forced volatilization.

Acknowledgments

This work is funded by the French National research Agency ANR through grant ANR-18-CE04-0004-01, project DECISIVE. We thank Olivier Grauby for the mineralogical analyses and Gwenaël Imfeld and Fabrice Martin-Laurent for helpful comments on the manuscript.

ASSOCIATED CONTENT

Supplementary Information

Scheme and picture of laboratory setup, characterization of the aquifer sediment, details on linearity of IRMS, isotope effects for phase changes of toluene and propane-2-ol, additional data for hydrogen isotope experiments and PHREEQC model for volatilization. This material is available free of charge on the Journal web site.

References

Aelion, C., Kirtland, B., 2000. Physical versus biological hydrocarbon removal during air sparging and soil vapor extraction. Environ. Sci. Technol. 34, 3167-3173.

Allen-King, R., Grathwohl, P., Ball, W., 2002. New modeling paradigms for the sorption of hydrophobic organic chemicals to heterogeneous carbonaceous matter in soils, sediments, and rocks. Adv. in Water Resour. 25, 985-1016.

Balseiro-Romero, M., Monterroso, C., Casares, J., 2018. Environmental Fate of Petroleum Hydrocarbons in Soil: Review of Multiphase Transport, Mass Transfer, and Natural Attenuation Processes. Pedosphere 28, 833-847.

Bartell, L. S., Roskos, R., 1966. Isotope effects on molar volume and surface tension - simple theoretical model and experimental data for hydrocarbons. J. Chem. Phys. 44, 457-463.

Bouchard, D., Hunkeler, D., Gaganis, P., Aravena, R., Höhener, P., Kjeldsen, P., 2008 a. Carbon isotope fractionation during migration of petroleum hydrocarbon vapors in the unsaturated zone: field experiment at Værløse Airbase, Denmark, and modeling. Environ. Sci. Technol. 42, 596-601.

Bouchard, D., Höhener, P., Hunkeler, D., 2008 b. Carbon isotope fractionation during volatilization of petroleum hydrocarbons and diffusion across a porous medium: a column experiment. Environ. Sci. Technol. 42, 7801–7806.

Bouchard, D., Marchesi, M., Madsen, E., DeRito, C., Thomson, N., Aravena, R., Barker, J., Buscheck, T., Kolhatkar, R., Daniels, E., Hunkeler, D., 2018. Diagnostic Tools to Assess Mass

340 Removal Processes During Pulsed Air Sparging of a Petroleum Hydrocarbon Source Zone.
341 Ground Water Monit. and Remediat. 38, 29-44.

342 Broholm, M. Christophersen, M., Maier, U., Stenby, E. , Höhener, P., Kjeldsen, P. 2005.
343 Compositional evolution of the emplaced fuel source experiment in the vadose zone field
344 experiment at Airbase Værløse, Denmark. Environ. Sci. Technol., 39: 8251-63.

345 Brusturean, G., Todinca, T., Perju, D., Carre, J., Bourgos, J., 2007. Soil clean up by venting:
346 Comparing between modelling and experimental voc removal results. Environ. Technol. 28,
347 1153-1162.

348 Delle Site, A., 2001. Factors affecting sorption of organic compounds in natural sorbent/water
349 systems and sorption coefficients for selected pollutants. A review. J. Phys. Chem. Ref. Data 30,
350 187-439.

351 Elsner, M., 2010. Stable isotope fractionation to investigate natural transformation mechanisms
352 of organic contaminants: principles, prospects and limitations. J. Environ. Monitor. 12, 2005-
353 2031.

354 Grathwohl, P., Reinhard, M., 1993. Desorption of trichloroethylene in aquifer material - rate
355 limitation at the grain scale. Environ. Sci. Technol. 27, 2360-2366.

356 Harrington, R. R., Poulson, S. R., Drever, J. I., Colberg, P. J. S., Kelly, E. F., 1999. Carbon
357 isotope systematics of monoaromatic hydrocarbons: vaporization and adsorption experiments.
358 Org. Geochem. 30, 765-775.

359 Höhener, P., Bouchard, D., Hunkeler, D. Stable isotopes as a tool for monitoring the
360 volatilization of non-aqueous phase liquids from the unsaturated zone. In: L. Candela, I. Vadillo

and F.J. Elorza (Editors), Advances in Subsurface Pollution of Porous Media. Indicators, Processes and Modelling. IAH Selected Papers on Hydrogeology, Vol. 14. CRC Press, Taylor and Francis Group, Boca Raton, pp. 123-135.

Höhener, P., Yu, X., 2012. Stable carbon and hydrogen isotope fractionation of dissolved organic groundwater pollutants by equilibrium sorption. J. Contam. Hydrol. 129/130, 54-61.

Imfeld, G., Kopinke, F. D., Fischer, A., Richnow, H. H., 2014. Carbon and hydrogen isotope fractionation of benzene and toluene during hydrophobic sorption in multistep batch experiments. Chemosphere 107, 454-461.

Julien, M., Höhener, P., Robins, R. J., Parinet, J., Remaud, G. S., 2017. Position-Specific 13C Fractionation during Liquid-Vapor Transition is Correlated to the Strength of Intermolecular Interaction in the Liquid Phase. J. Phys. Chem. 121, 5810-5817.

Kiss, I., Jakli, G., Illy, H., 1972. Isotope effects on vapour pressure. Acta Chim. Hung. 71, 59-74.

Kopinke, F. D., Georgi, A., Voskamp, M., Richnow, H. H., 2005. Carbon isotope fractionation of organic contaminants due to retardation on humic substances: Implications for natural attenuation studies in aquifers. Environ. Sci. Technol. 39, 6052-6062.

Kuder, T., Philp, P., Allen, J., 2009. Effects of volatilization on carbon and hydrogen isotope ratios of MTBE. Environ. Sci. Technol. 43, 1763-1768.

Morasch, B., Schink, B., Richnow, H., Meckenstock, R., 2001. Stable hydrogen and carbon isotope fractionation during microbial toluene degradation. mechanistic and environmental aspects. Appl. Environ. Microbiol. 67, 4842-4849.

Ostendorf, D., Kampbell, D., 1990. Bioremediated soil venting of light hydrocarbons. Hazard. Waste Hazard. Mater. 7, 319-335.

Ponsin, V., Maier, J., Guelorget, Y., Hunkeler, D., Bouchard, D., Villavicencio, H., Höhener, P., 2015. Documentation of time-scales for onset of natural attenuation in an aquifer treated by a crude-oil recovery system. Sci. Tot. Environ. 512-513, 62-73.

Rathfelder, K., Lang, J., Abriola, L., 1995. Soil Vapor Extraction And Bioventing - Applications, Limitations, and Future-Research Directions. Rev. Geophys. 33, 1067-1081.

Schuth, C., Taubald, H., Bolano, N., Maciejczyk, K., 2003. Carbon and hydrogen isotope effects during sorption of organic contaminants on carbonaceous materials. J. Contam. Hydrol. 64, 269-281.

Slater, G. F., Ahad, J. M. E., Lollar, B. S., Allen-King, R., Sleep, B., 2000. Carbon isotope effects resulting from equilibrium sorption of dissolved VOCs. Anal. Chem. 72, 5669-5672.

Thullner, M., Centler, F., Richnow, H. H., Fischer, A., 2012. Quantification of organic pollutant degradation in contaminated aquifers using compound specific stable isotope analysis - Review of recent developments. Org. Geochem. 42, 1440-1460.

USGS, 2002. PHREEQC: A computer program for speciation, batch-reaction, one-dimensional transport, and inverse geochemical calculations. Geological Survey of the United States, http://wwwbrr.cr.usgs.gov/projects/GWC_coupled/phreeqc/.

Vogt, C., Dorer, C., Musat, F., Richnow, H. H., 2016. Multi-element isotope fractionation concepts to characterize the biodegradation of hydrocarbons from enzymes to the environment. Curr. Opin. Biotechnol. 41, 90-98.

Figure Captions

Figure 1: A) *Evolution of concentration (expressed as amplitude, circles) and of carbon isotope ratio (squares) during volatilization of toluene from unsaturated humid sandy aquifer sediment.* ***B)*** *Evolution of the hydrogen isotope ratios and vapor concentrations expressed as amplitudes of mass 2 during desorption of toluene from sandy aquifer sediment.*

Figure 2: *Vapor concentration expressed as amplitude mass 44 (A) and carbon stable isotope change (B) during volatilization/desorption of toluene from unsaturated sandy sediment with distinct initial masses of toluene. Flow rates varied from 6 to 12 mL* min^{-1}.

Figure 3: *Evolution of concentration expressed as amplitude, and of Carbon (A) and Hydrogen (B) isotope during volatilization/desorption of propan-2-ol from unsaturated sandy aquifer sediment.*

Figure 4: *Results for* ^{13}C *of the numerical model, with variation of 4 model parameters: A) toluene mass B) number of stirred cells forming the columns C) dispersivity, and D) vapor-liquid isotope effect VPIE. See Tab. S5 for other parameters. The vapor concentration at the column end is always at saturation and drops to zero after the last data point.*

Figure 5: *Magnitude of isotope shifts observed in this work for toluene compared to isotope shifts by other processes as reviewed in* (Bouchard et al., 2018).

422 Figure 1:

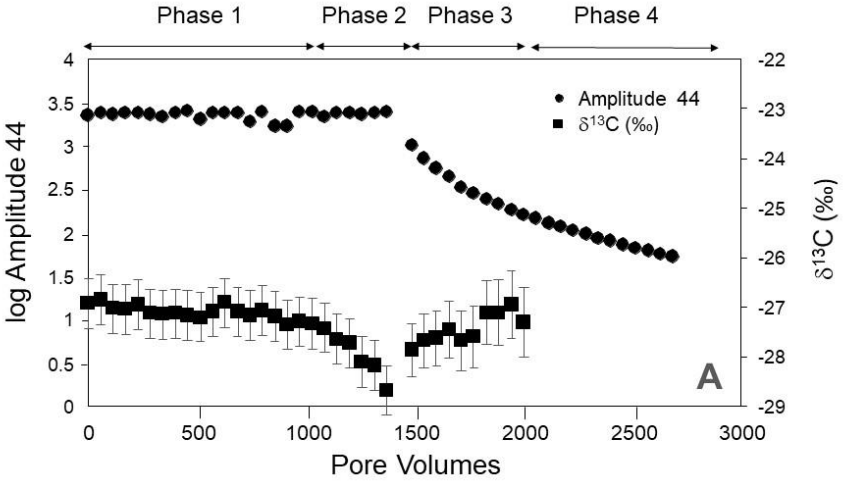

423

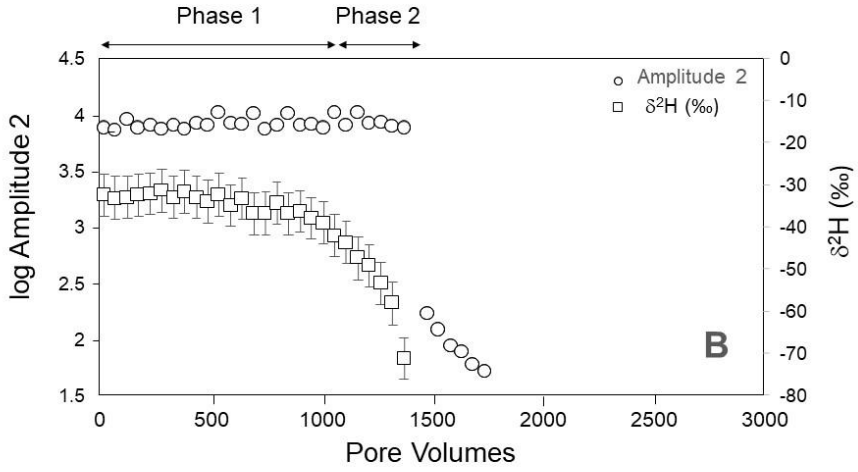

424

425 Figure 2:

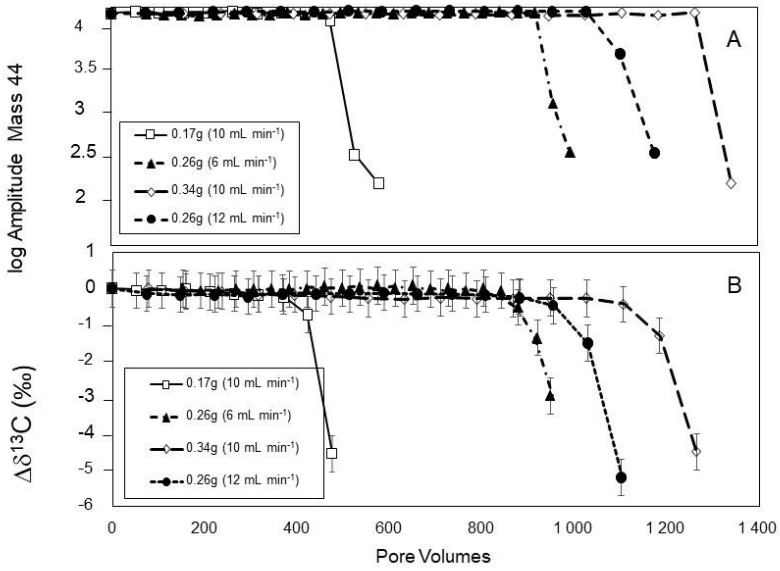

426

427 Figure 3:

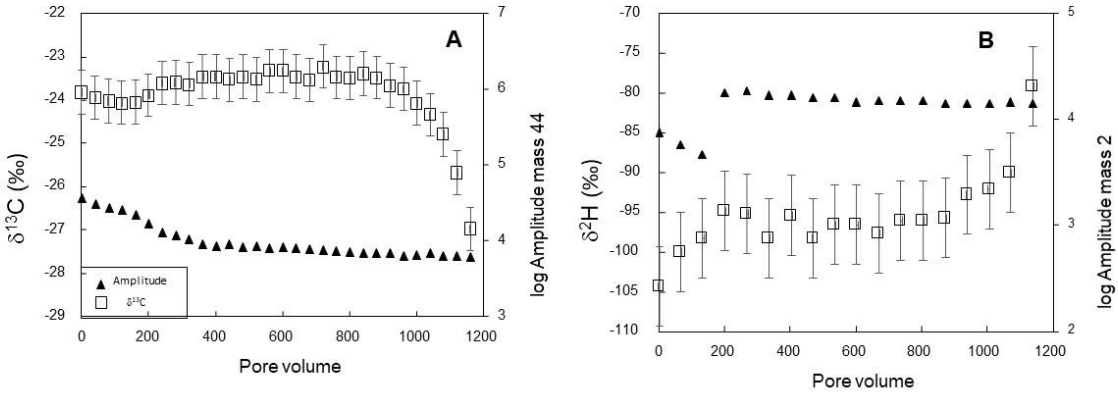

428

429 Figure 4:

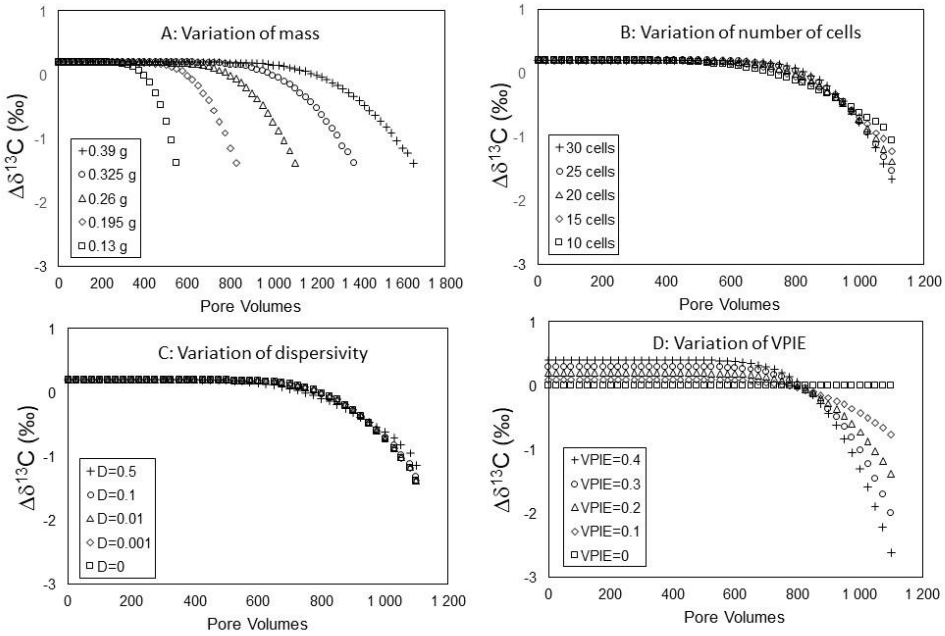

430

431

Figure 5:

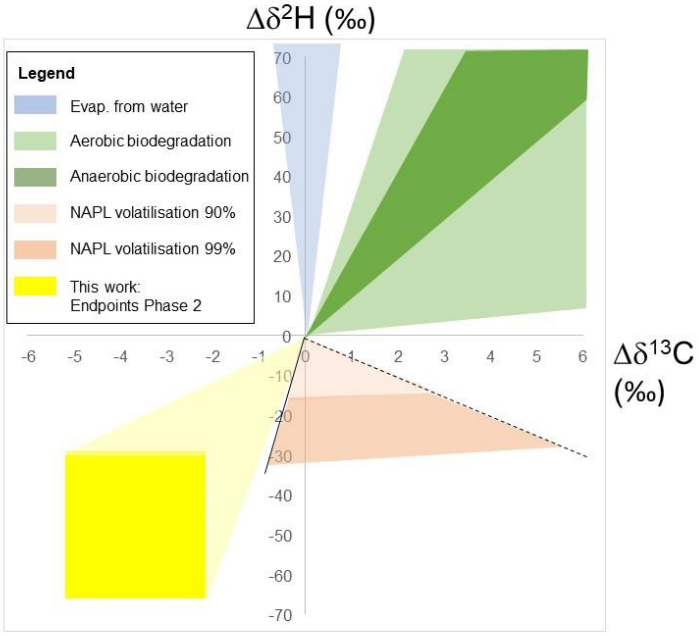
Δδ²H (‰)
Legend
Evap. from water
Aerobic biodegradation
Anaerobic biodegradation
NAPL volatilisation 90%
NAPL volatilisation 99%
This work:
Endpoints Phase 2
70
60
50
40
30
20
10
0
-10
-20
-30
-40
-50
-60
-70
-6
-5
-4
-3
-2
-1
0
1
2
3
4
5
6
Δδ¹³C
(‰)